

An experimental investigation of rapid boiling of CO₂

S. Tosse · K. Vaagsaether · D. Bjerketvedt

Received: 30 October 2013 / Revised: 21 August 2014 / Accepted: 26 August 2014 / Published online: 27 September 2014
© The Author(s) 2014. This article is published with open access at Springerlink.com

Abstract Storage of pressurized liquified gases is a growing safety concern in many industries. Knowledge of the thermodynamics and kinetics involved in the rapid depressurization and evaporation of such substances is key to the design and implementation of effective safety measures in storage and transportation situations. In the present study, experiments on the rapid depressurization of liquid CO₂ are conducted in a vertical transparent shock tube which enables the observation of evaporation waves and other structures. The depressurization was initiated by puncturing a membrane in one end of the tube. The thermodynamic mechanisms that govern the evaporation process are not unique to CO₂, and the same principles can be applied to any liquified gas. The experiments were photographed by a high-speed camera. Evaporation waves propagating into the liquid were observed, traveling at a near constant velocity on the order of 20–30 m/s. A contact surface between the vapor and the liquid–vapor mixture was also observed, accelerating out of the tube. Pressure readings in the tube suggest that the evaporation wave could be similar to a spinodal decomposition wave, but further experiments are needed to confirm this. When the membrane was in direct contact with the liquified CO₂, some indications of homogeneous nucleation were observed.

Keywords CO₂ · Phase transition · Evaporation waves · Two-phase flow

1 Introduction

Accidental explosions involving the rapid boiling of liquified gases are of great concern in process safety. Such events are sometimes referred to as Boiling Liquid Expanding Vapor Explosions (BLEVEs). A BLEVE can occur in the storage and transportation of high pressure liquified gases such as LPG or CO₂. To prevent and mitigate BLEVE accidents, detailed knowledge about the thermodynamic process is needed. There are several definitions of the term BLEVE, an overview of which is provided by Abbasi and Abbasi [1]. Some of the definitions involve complete failure of the vessel. Based on such a definition, the present experiments do not qualify as a BLEVE. However, the research is still relevant for BLEVE-type scenarios as the governing kinetics and thermodynamics is the same.

Evaporation waves in a superheated liquid (Refrigerant 12 and 114) were observed by Hill [2]. Simoes-Moreira and Shepherd [3] also performed a series of experiments with superheated dodecane. Reinke and Yadigaroglu [4] did a series of experiments with explosive vaporization in propane, butane and refrigerant R-134a. Bjerketvedt et al. [5] conducted a series of small-scale experiments with CO₂ BLEVEs. Some work has been done to develop numerical models that are capable of describing evaporation waves. Saurel et al. [6] developed a Godunov method for compressible multiphase flow that was later applied to the subject of phase transition in metastable liquids [7]. They were able to qualitatively reproduce the evaporation front velocities measured by Simoes-Moreira and Shepherd. Zein et al. [8] used the same numerical model to reproduce the results of Simoes-

Communicated by G. Ciccarelli.

This paper is based on work that was presented at the 24th International Colloquium on the Dynamics of Explosions and Reactive Systems, Taipei, Taiwan, July 28–August 2, 2013.

S. Tosse (✉) · K. Vaagsaether · D. Bjerketvedt
Faculty of Technology, Telemark University College,
Kjolnes Ring 56, 3918 Porsgrunn, Norway
e-mail: sindre.tosse@hit.no

Moreira and Shepherd with better accuracy. In recent years, there have also been several attempts to model BLEVE-type scenarios [9–11]. The knowledge of detailed thermodynamics and kinetics is important in the validation of such models.

The scope of the experimental work is to provide insight into the overall thermodynamics and kinetics that govern the evaporation process in superheated CO_2 . Velocities of evaporation waves and contact surfaces as well as pressure readings are important in providing such insight. The results will also function as a basic reference for a numerical model capable of describing the boiling mechanisms in superheated CO_2 . Validation of such a model will require more detailed experimental work, particularly with pressure readings at several points in the tube (only two pressure transducers were used in the present setup). Lastly, the present study will serve as a reference if a new experimental rig is constructed.

It is common to use term boiling for the phase transition that takes place when vapor bubbles form within a liquid body or at an interface with a solid body. In the present experimental work, there is often no clear liquid surface or body but rather a mixture of vapor and liquid. The term evaporation waves is described by Simoes-Moreira [12] as 'processes that may occur under certain conditions in which a metastable or superheated liquid undergoes a sudden phase transition in a narrow and observable region [...].' We use this term when such phenomena are observed and the term boiling for other liquid–gas phase transitions.

2 Experimental setup

The experiment was carried out in a vertically oriented clear Lexan tube partly filled with liquid CO_2 . A schematic illustration of the tube is provided in Fig. 1. The visible portion of the tube was 32 cm in length. The inner-diameter of the tube was 9 mm and the outer-diameter was 12 mm. One end of the tube was a membrane which was punctured by a needle. Two layers of Mylar sheet were used as the membrane material. The experiment was photographed using a high-speed camera (Photron APX-RS) at 16,000 frames per second ($64 \times 1,024$ pixels), which allowed visual tracking of the various fronts and bulk boiling. The tube was illuminated from the front by white light. Some experiments were done using back lighting, but the light was not able to penetrate the two-phase region. In addition to the high-speed camera, two Kulite XT-190 pressure transducers (P_1 and P_2 in Fig. 1) were used to record the pressure inside the tube. The distance between the two pressure transducers was 43.5 cm. The first series of experiments were conducted with the membrane placed at the top of the tube. The vertical orientation of the tube was reversed in the second series, so that the membrane was at the bottom.

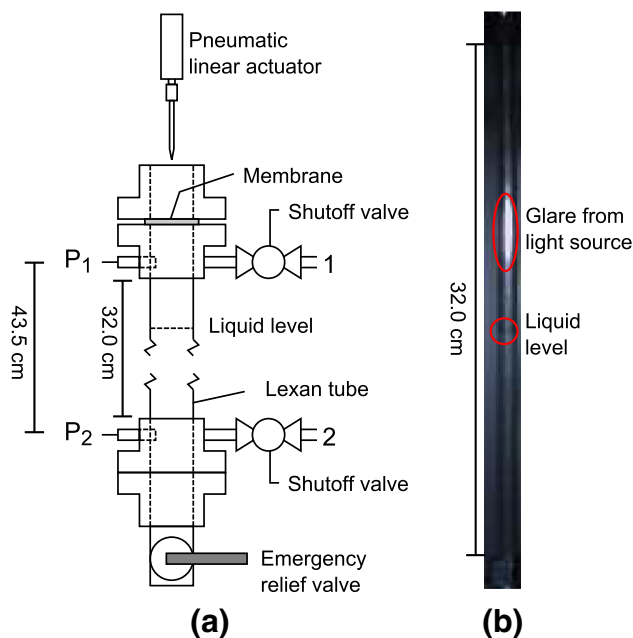


Fig. 1 **a** Schematic illustration of the shock tube with vapor side penetration (not to scale). The tube was filled at the inlet (2), while (1) was used for controlled pressure relief to allow liquid CO_2 to fill the tube. P_1 and P_2 are pressure transducers. The distance from P_1 to P_2 was 43.5 cm, and the transparent part of the tube was 32.0 cm in length. **b** Example high-speed shot of the tube filled with liquid CO_2 . This is the total field of view of the camera. Note that the length of 32.0 cm indicated in both **a** and **b** is the part of the tube that is shown in the photographs in the result section

The tube was filled through an inlet valve at the bottom of the tube using liquid CO_2 from a gas bottle with a riser tube. Careful pressure relief at the top of the tube allowed the liquid CO_2 to fill the tube to the desired level. When the fill (1) and relief (2) valves shown in Fig. 1 were closed, the thermodynamic state inside the tube was assumed to be in equilibrium between the liquid and vapor.

3 Experimental results and discussion

The experimental results are provided for two cases. In the first case, the membrane was placed at the top of the tube so that the vapor head space was directly below the membrane. In the second case, the vertical orientation of the tube was reversed so that liquid was located directly above the membrane. The high-speed images are displayed as a series of isochronously spaced images, which allow the fronts to be easily tracked. The front velocities are found by polynomial curve fitting of the front position versus time. All images are cropped to show only the visible portion of the tube, with a height of 32.0 cm. The pixel width was 0.35 mm/px. Visual tracking of fronts is possible, but as the front position is not always clear, some uncertainty in the calculated

velocities should be expected. The uncertainties were estimated by varying the gradient of the velocity to fit within the front region. Due to the curvature of the tube and the lack of magnification, it was not possible to observe the evaporation front structure.

3.1 Vapor side membrane placement

Figure 2 shows the experimental results when the shock tube is filled with liquid CO₂ up to 45 % of the height between P₁ and P₂. The pressure time histories in Fig. 2 show a 1.83 ± 0.09 ms delay between the first pressure drop in the upper and the lower pressure transducer. This corresponds to a mean speed of sound of 238 ± 12 m/s. As a reference, at 5.5 MPa saturated conditions and a liquid fill level of 45 %, the Span–Wagner equation of state [13] gives a mean speed of sound of 248 m/s (198.0 m/s in the vapor and 356.8 m/s in the liquid phase). The Span–Wagner speed of sound of each phase has been plotted as the dashed red line in Fig. 2 to illustrate the predicted path of the first rarefaction wave.

From the pressure drop at P₁, there is a time delay of 0.8 ms until any visual changes occur in the tube. Some of this delay can be explained by the 5.75 cm gap between the

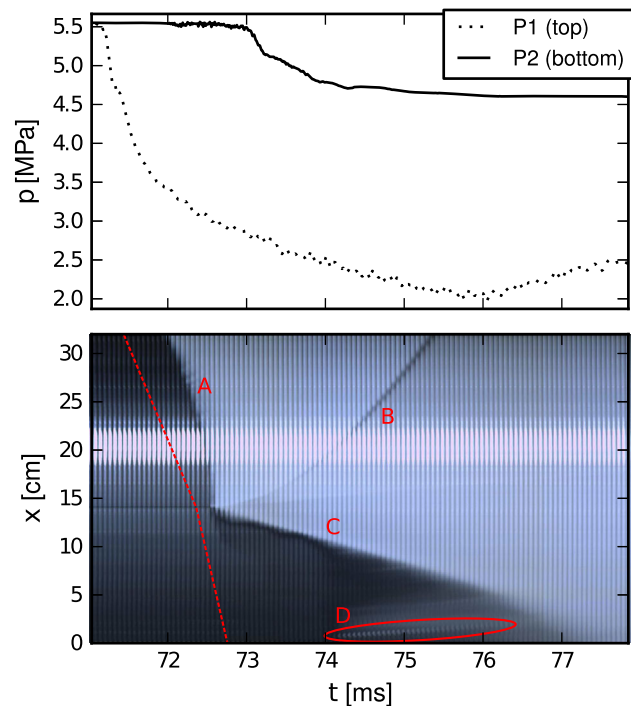


Fig. 2 Experimental results with vapor side membrane penetration. P₁ and P₂ refer to Fig. 1a. The time-scale is relative to the trigger mechanism of the membrane penetration device. The red dotted line is the trajectory of the first rarefaction wave traveling at the speed of sound as given by the Span–Wagner equation of state. A Condensation wave. B Vapor–mixture interface. C Evaporation wave. D Bubbles in liquid

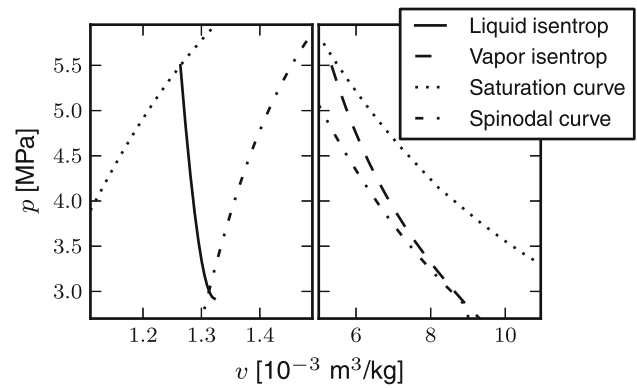


Fig. 3 Isentropic expansion from the initial conditions of saturation at 5.5 MPa in p - v space (Span–Wagner equation of state). The liquid isentrop intersects the spinodal curve at 3.0 MPa. The spinodal curve is defined by $\left(\frac{\partial p}{\partial v}\right)_T = 0$

pressure transducer and the upper end of the visible portion of the tube, but it is likely that the pressure in the tube drops prior to the appearance of the changes. This implies that the vapor becomes sub-cooled prior to the visual changes. As a reference, isentropic expansion of vapor from the known initial conditions to 3.5 MPa using the Span–Wagner equation of state yields a sub-cooled vapor temperature of 262 K. Since this is well above the triple-point temperature of CO₂ (216.6 K), it is safe to assume that the white front that propagates downwards into the vapor from $t = 72$ ms (line A in Fig. 2) consists of condensed droplets and not solid particles.

At 1.4 ms after the initial pressure drop at P₁, the liquid starts to boil at the interface. The boiling propagates as a front into the liquid (line C in Fig. 2). At the same time, a front is seen accelerating upward into the vapor phase (line B in Fig. 2). This is most likely the contact surface between the the vapor and the liquid–vapor mixture that is produced by the boiling liquid. The evaporation front and the contact surface are plotted in Fig. 4. The evaporation front is fitted with a constant velocity of 25 ± 1 m/s and the contact surface is fitted with a constant acceleration of 40.8 ± 0.5 km/s². These fronts are well known phenomena in the context of evaporation waves, and are described among others by Pinhasi et al. [9]. The pressure at the top of the tube increases slightly after the contact surface passes, up to a level of 2.6 MPa. Using the Span–Wagner equation of state, the isentrop from the initial 5.5 MPa at saturated conditions intersects the spinodal curve at 3.0 MPa as shown in Fig. 3. While it is impossible to determine the exact pressure in the liquid–vapor mixture zone with the current experimental setup, it is possible that it is on the same order as the top pressure after the contact surface passes. If this is the case, the evaporation front could be close to a spinodal decomposition wave. It should also be noted that the increase in pressure following the exit of the contact surface could be the result of changed choking conditions at the tube exit. When the two-phase mixture is

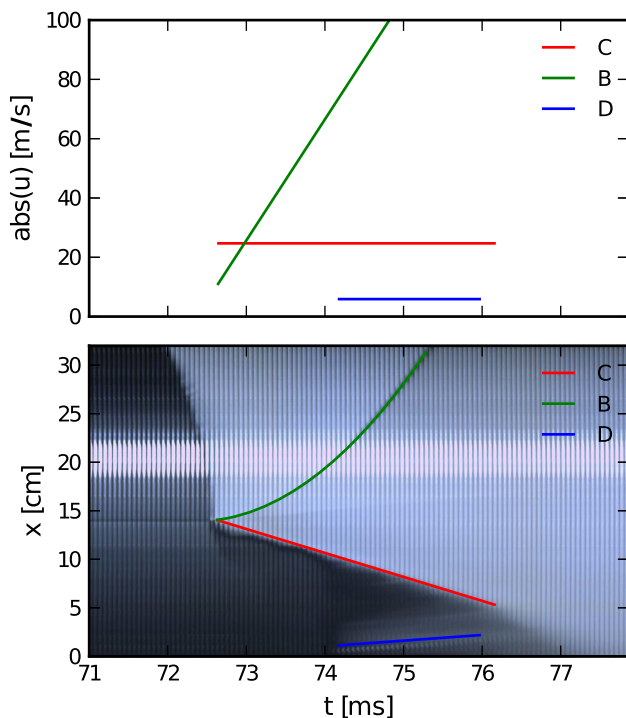


Fig. 4 Curve fittings of front positions and velocities from Fig. 2 plotted with time. *C* Evaporation wave. *B* Vapor–mixture interface. *D* Bubbles in liquid

subject to the sudden pressure drop at the tube exit, some of the liquid will evaporate.

After $t = 74$ ms, the liquid appears to be boiling at the bottom of the tube (region D in Fig. 2). At this point, P_2 is stabilized at roughly 4.6 MPa. The pressure is most likely stabilized because of the boiling process in the liquid. The boiling appears to be non-homogeneous so it is most likely caused by impurities at the wall or at the tube end. Some structures are observed moving upwards. In Fig. 4, these structures are fitted to a constant velocity of 6.0 ± 0.5 m/s. This may be an indication of bulk fluid velocity.

3.2 Liquid side membrane placement

In these experiments, the membrane was placed at the bottom of the tube. Figure 5 shows the experimental results with the tube filled with liquid CO_2 up to the top of the visible portion. The dashed red line in the figure is the predicted path of the first rarefaction wave based on the Span–Wagner speed of sound. At 2.0 ms after the first drop in P_1 , the first sign of boiling appears. It is interesting to note that the boiling appears to be initiated at the liquid–vapor interface at the top even though the membrane is located at the bottom of the tube. The liquid also boils at the membrane side, but the velocity of liquid flowing out of the tube is greater than that of the boiling, so the lower evaporation wave is never

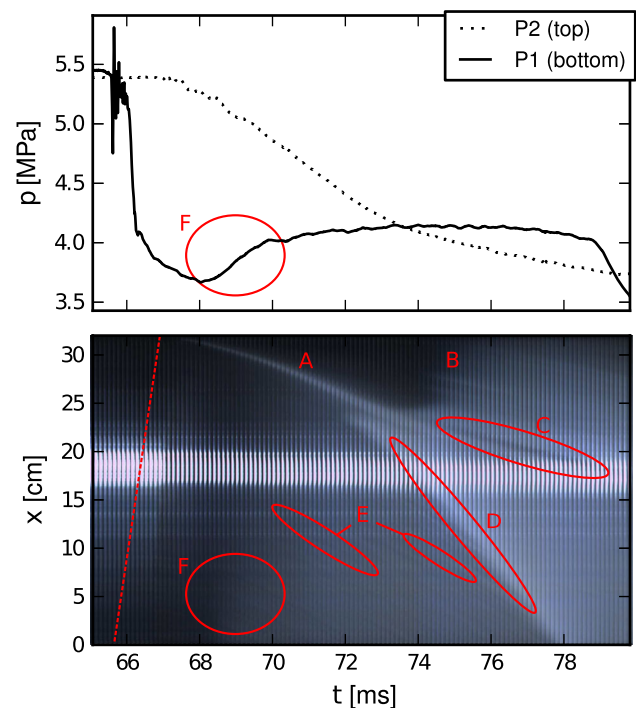


Fig. 5 Experimental results with liquid side membrane penetration. P_1 and P_2 refer to Fig. 1a. The time-scale is relative to the trigger mechanism of the membrane penetration device. The red dotted line is the trajectory of the first rarefaction wave traveling at the speed of sound as given by the Span–Wagner equation of state. *A* Liquid–vapor interface. *B* Condensation wave. *C* Vapor–mixture interface. *D* Evaporation wave. *E* Bubbles in liquid. *F* Homogeneous boiling

visible. The liquid–vapor interface is accelerating downward (line A in Fig. 5). The white area at the interface is expanding from barely visible at $t = 68$ ms to 1 cm in height at $t = 72$ ms. The white area could be liquid boiling at a low rate. At $t = 75.5$ ms the vapor phase becomes opaque (line B in Fig. 5). This is assumed to be caused by a condensation process in the sub-cooled vapor like in the previous setup. The condensation appears to be initiated at the liquid–vapor interface and propagates upward into the vapor for some time before the rest of the vapor condensates simultaneously. The liquid–vapor interface continues downward, but appears to decelerate (region C in Fig. 5). Around $t = 72$ ms, a new front appears (region D in Fig. 5) and accelerates downward into the liquid.

The accelerating front is most likely an evaporation wave similar to the one observed in the first series of experiments. Region C is then possibly a mixture–vapor contact surface. The difference is that in the first series, the liquid flow velocity was in the opposite direction of the evaporation wave. Here, the liquid phase is flowing out of the tube at an unknown, possibly increasing flow velocity. Figure 6 shows curve fittings of the liquid–vapor interface and the evaporation wave.

With careful consideration of Fig. 5, one can observe some white streaks in the liquid phase (region E in Fig. 5), cor-

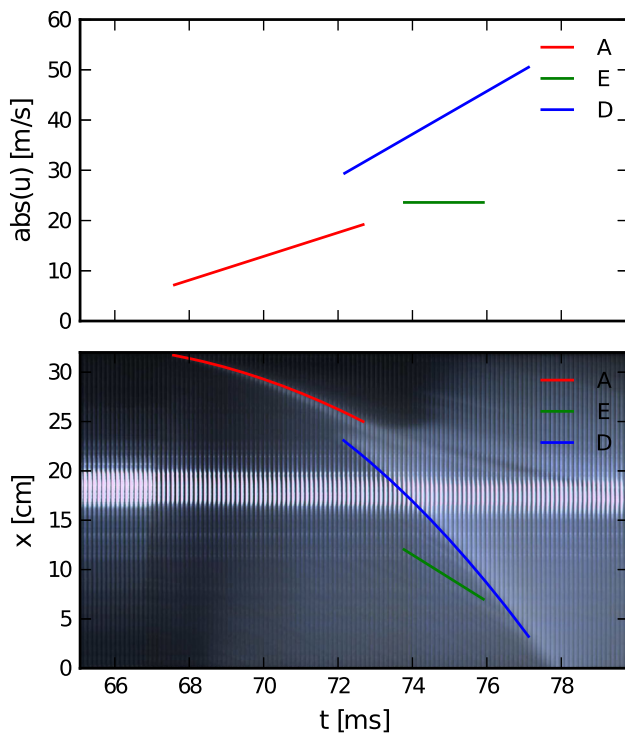


Fig. 6 Curve fittings of front positions and velocities from Fig. 5 plotted with time. *A* Liquid–vapor interface. *E* Bubbles in liquid. *D* Evaporation wave

responding to a velocity on the order of 20 m/s (line E in Fig. 6). Note that these streaks are barely visible. They are most likely small structures (bubbles) in the liquid that act as tracers from which the liquid velocity can be inferred, but the nature of the observations makes further investigations necessary to confirm this.

Between $t = 68$ ms and $t = 70$ ms, there is an increase in the bottom pressure as well as a distinct change in brightness in the liquid (region F in Fig. 5). The change appears to be homogeneous. This may be an indication of homogeneous nucleation.

Due to various reasons, only one complete data set exists for the setup with the membrane placed at the bottom of the tube. This implies that the repeatability of the results presented in this section is unknown and that these results may be unique.

4 Conclusion

- The current setup of high-speed photography is capable of capturing the propagation of evaporation waves and contact surfaces in a tube with liquid CO₂. Rarefaction waves were not observed.
- The small diameter of the tube makes it difficult to observe detailed structures, especially in the cross-sectional direction.

- When the membrane was burst on the vapor (top) side, an evaporation wave was observed that traveled into the liquid with a velocity on the order of 20–30 m/s. Another front, assumed to be the contact surface between the vapor and the liquid–vapor mixture, was also observed accelerating out of the tube.
- When the membrane was burst on the liquid (bottom) side, an evaporation wave and a contact surface still appeared at the top of the tube, but further experiments are needed to determine the front velocities. Some indications of homogeneous nucleation were observed in the superheated liquid.

Due to the lack of pressure measurements inside the tube, it is hard to say anything about the thermodynamic states in the observed structures. Knowledge about such states is critical for understanding the governing mechanisms in a BLEVE. A new experimental setup is needed to provide pressure and temperature readings at several places in the tube. Such a setup should also have a square tube profile or a much larger tube diameter to capture detailed structures in the boiling front.

Open Access This article is distributed under the terms of the Creative Commons Attribution License which permits any use, distribution, and reproduction in any medium, provided the original author(s) and the source are credited.

References

1. Abbasi, T., Abbasi, S.A.: The boiling liquid expanding vapour explosion (BLEVE): mechanism, consequence assessment, management. *J. Hazard. Mater.* **141**, 489–519 (2007). doi:[10.1016/j.jhazmat.2006.09.056](https://doi.org/10.1016/j.jhazmat.2006.09.056)
2. Hill, L.G.: An experimental study of evaporation waves in a superheated liquid. Dissertation (Ph.D.), California Institute of Technology (1990)
3. Simoes-Moreira, J.R., Shepherd, J.E.: Evaporation waves in superheated dodecane. *J. Fluid Mech.* **382**, 63–86 (1999). doi:[10.1017/S0022112098003796](https://doi.org/10.1017/S0022112098003796)
4. Reinke, P., Yadigaroglu, G.: Explosive vaporization of superheated liquids by boiling fronts. *Int. J. Multiph. Flow* **27**, 1487–1516 (2001). doi:[10.1016/S0301-9322\(01\)00023-4](https://doi.org/10.1016/S0301-9322(01)00023-4)
5. Bjerketvedt, D., Egeberg, K., Ke, W., Gaathaug, A., Vaagsaether, K., Nilsen, S.H.: Boiling liquid expanding vapour explosion in CO₂ small scale experiments. *Energy Procedia* **4**, 2285–2292 (2011). doi:[10.1016/j.egypro.2011.02.118](https://doi.org/10.1016/j.egypro.2011.02.118)
6. Saurel, R., Abgrall, R.: A multiphase Godunov method for compressible multfluid and multiphase flows. *J. Comput. Phys.* **150**, 425–467 (1999). doi:[10.1006/jcph.1999.6187](https://doi.org/10.1006/jcph.1999.6187)
7. Saurel, R., Petitpas, F., Abgrall, R.: Modelling phase transition in metastable liquids: application to cavitating and flashing flows. *J. Fluid Mech.* **607**, 313–350 (2008). doi:[10.1017/S0022112008002061](https://doi.org/10.1017/S0022112008002061)
8. Zein, A., Hantke, M., Warnecke, G.: Modeling phase transition for compressible two-phase flows applied to metastable liquids. *J.*

- Comput. Phys. **229**, 2964–2998 (2010). doi:[10.1016/j.jcp.2009.12.026](https://doi.org/10.1016/j.jcp.2009.12.026)
9. Pinhasi, G.A., Ullmann, A., Dayan, A.: 1D plane numerical model for boiling liquid expanding vapor explosion (BLEVE). *Int. J. Heat Mass Transf.* **50**, 4780–4795 (2007). doi:[10.1016/j.ijheatmasstransfer.2007.03.016](https://doi.org/10.1016/j.ijheatmasstransfer.2007.03.016)
 10. Voort, M.M., Berg, A.C., Roekaerts, D.J.E.M., Xie, M., Bruijn, P.C.J.: Blast from explosive evaporation of carbon dioxide: experiment, modeling and physics. *Shock Waves* **22**, 129–140 (2012). doi:[10.1007/s00193-012-0356-0](https://doi.org/10.1007/s00193-012-0356-0)
 11. Xie, M.: Thermodynamic and Gasdynamic Aspects of a Boiling Liquid Expanding Vapour Explosion. PhD Thesis, Delft University of Technology, The Netherlands (2013)
 12. Simoes-Moreira, J.R.: Oblique evaporation waves. *Shock Waves* **10**, 229–234 (2000). doi:[10.1007/s001930000050](https://doi.org/10.1007/s001930000050)
 13. Span, R., Wagner, W.: A new equation of state for carbon dioxide covering the fluid region from the triple-point temperature to 1100 K at pressures up to 800 MPa. *J. Phys. Chem. Ref. Data* **25**, 1509–1596 (1996)